Effects of nuclear fragmentation on single particle and collective motions at low energy*

C. Barbieri†

TRIUMF, 4004 Wesbrook Mall, Vancouver, British Columbia, Canada V6T 2A3

W. H. Dickhoff‡

Department of Physics, Washington University, St.Louis, Missouri 63130, USA

The Faddeev technique is employed to study the influence of both particle-particle and particle-hole phonons on the one-hole spectral function of ^{16}O. The formalism includes the effects of nuclear fragmentation and accounts for collective excitations at a random phase approximation (RPA) level. The latter are subsequently summed to all orders by the Faddeev equations to obtain the nucleon self-energy. The results indicate that the characteristics of hole fragmentation are related to the low-lying states of ^{16}O and an improvement of the description of this spectrum is required to understand the details of the experimental strength distribution. A first calculation to improve on this includes the mixing of two-phonon configuration with particle-hole ones. It is seen that this allows to understand the formation of excited states which cannot be described by the RPA approach.

PACS numbers:

I. INTRODUCTION

The studies of spectral distribution in nuclei during the last decade has made available the best information to date regarding correlations in nuclear systems [1]. Experimentally, $(e, e'p)$ reactions have provided precise information for spectroscopic factors of states close to the Fermi energy [2, 3] in finite nuclei. Moreover, information on the tail of the spectral distribution at high missing energies and momenta, generated by short-range correlations (SRC), has recently become available [4]. The observed spectroscopic factors have been reproduced for selected nuclei, such as ^{48}Ca and ^{90}Zr [5], and a particularly successful comparison between theory and experiment has been obtained for ^{7}Li [6]. In all these calculations, the effects of configuration mixing at low energy was taken properly into account. Besides, the effects of SRC have been investigated for different systems and are known to give a constant reduction of the spectroscopic strength of 10-15%, for the fragments close to the Fermi energy [7–9].

For the case of ^{16}O, there still exists a substantial disagreement between experiment [3] and theory [7, 8, 10–12]. The latter has been able to explain only a part of the quenching of spectroscopic factors for proton knockout from the p-shell. The results of Refs. [10, 11] show that the reasons for this discrepancy have to be looked for in terms of long-range correlations (LRC) and in particular in the couplings of single-particle (sp) motion to low-energy collective excitations.

In this paper we report about the work done along this line in Refs. [12, 13] in order to approach

---

* Proceedings of the "10$^{\rm th}$ international conference on nuclear reaction mechanisms", Varenna, 9-13 June 2003.
†Electronic address: barbieri@triumf.ca; URL: http://www.triumf.ca/people/barbieri
‡Electronic address: wimd@wuphys.wustl.edu; URL: http://www.physics.wustl.edu/~wimd

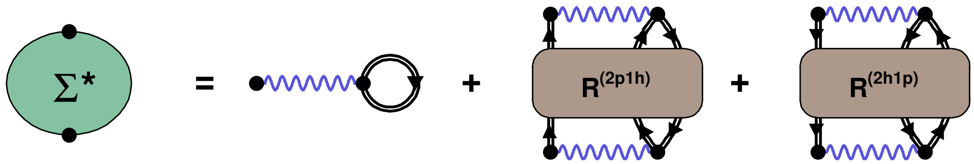

FIG. 1: Diagrams contributing to the irreducible self-energy Σ^*. The double lines represent a dressed propagator and the wavy lines correspond to G-matrix interactions. The first term is the Brueckner-Hartree-Fock potential while the others represent the 2p1h/2h1p or higher contributions that are approximated through the Faddeev TDA/RPA equations.

the above issues for ^{16}O. Sec. II describes the formalism employed to describe the coupling of particle-hole (ph), particle-particle (pp) and hole-hole (hh) collective excitation to the sp propagator. This is done by embedding the technique of Faddeev equations into the self-consistent Green's function formalism [14, 15]. The results of this calculation are given in Sec. III, where the effects of nuclear fragmentations and the random phase approximation (RPA) in the description of phonons are discussed. These calculations show that a proper description of the experimental spectral strength requires an improvement of the spectrum, that goes beyond the RPA approach. A first step in this direction is reported in Sec. IV, where the Bethe-Salpeter equation (BSE) is employed to pursue the improvement of the ph-RPA approach.

II. FADDEEV APPROACH THE CALCULATION OF THE SINGLE-PARTICLE GREEN'S FUNCTION

We consider the calculation of the sp Green's function

$$g_{\alpha\beta}(\omega) \;=\; \sum_n \frac{\left(\mathcal{X}_\alpha^n\right)^* \; \mathcal{X}_\beta^n}{\omega - \varepsilon_n^+ + i\eta} \;+\; \sum_k \frac{\mathcal{Y}_\alpha^k \; \left(\mathcal{Y}_\beta^k\right)^*}{\omega - \varepsilon_k^- - i\eta} \;, \tag{1}$$

from which both the one-hole and one-particle spectral functions, for the removal and addition of a nucleon, can be extracted. In Eq. (1), $\mathcal{X}_\alpha^n = \langle \Psi_n^{A+1} | c_\alpha^\dagger | \Psi_0^A \rangle$ ($\mathcal{Y}_\alpha^k = \langle \Psi_k^{A-1} | c_\alpha | \Psi_0^A \rangle$) are the spectroscopic amplitudes for the excited states of a system with $A+1$ ($A-1$) particles and the poles $\varepsilon_n^+ = E_n^{A+1} - E_0^A$ ($\varepsilon_k^- = E_0^A - E_k^{A-1}$) correspond to the excitation energies with respect to the A-body ground state. The one-body Green's function can be computed by solving the Dyson equation

$$g_{\alpha\beta}(\omega) = g^0_{\alpha\beta}(\omega) \;+\; \sum_{\gamma\delta} g^0_{\alpha\gamma}(\omega) \Sigma^*_{\gamma\delta}(\omega) g_{\delta\beta}(\omega) \;\;, \tag{2}$$

where the irreducible self-energy $\Sigma^*_{\gamma\delta}(\omega)$ acts as an effective, energy-dependent, potential. The latter can be expanded in a Feynman-Dyson series [16, 17] in terms the exact propagator $g_{\alpha\beta}(\omega)$, which itself is a solution of Eq. (2). In this expansion, $\Sigma^*_{\gamma\delta}(\omega)$ can be represented as the sum of a one-body Hartree-Fock potential and terms that describe the coupling between the sp motion and more complex excitations [18]. This separation is depicted by the diagrams of Fig. 1, where the last two diagrams are expressed in terms of the three-line irreducible propagator $R(\omega)$ which describes the propagation of at least 2h1p or 2p1h at the same time. It is at the level of $R(\omega)$ that the correlations involving interactions between different collective modes have to be included.

The SCGF approach consist of first solving the self-energy and the Dyson Eq. (2) in terms of a mean-field IPM propagator $g^0_{\alpha,\beta}(\omega)$. The (dressed) solution $g_{\alpha\beta}(\omega)$ is then used to evaluate the an improved self-energy, which then contains the effects of fragmentation. The whole procedure is

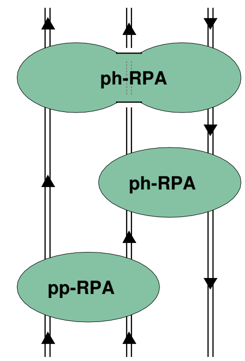

FIG. 2: Example of diagrams that are summed to all orders by means of the Faddeev equations.

iterated until self-consistency is reached. Baym and Kadanoff showed that a self-consistent solution of the above equation guarantees the fulfillment of the principal conservation laws [19].

A. Faddeev approach to the self-energy

In the following we are interested in describing the coupling of sp motion to ph and pp(hh) collective excitations of the system. All the relevant information regarding the latter are included in the Lehmann representations of the polarization propagator

$$\Pi_{\alpha\beta,\gamma\delta}(\omega) = \sum_{n\neq 0} \frac{\langle \Psi_0^A | c_\beta^\dagger c_\alpha | \Psi_n^A \rangle \, \langle \Psi_n^A | c_\gamma^\dagger c_\delta | \Psi_0^A \rangle}{\omega - (E_n^A - E_0^A) + i\eta} - \sum_{n\neq 0} \frac{\langle \Psi_0^A | c_\gamma^\dagger c_\delta | \Psi_n^A \rangle \, \langle \Psi_n^A | c_\beta^\dagger c_\alpha | \Psi_0^A \rangle}{\omega - (E_0^A - E_n^A) - i\eta} \, , \tag{3}$$

that describes the excited states in the system with A particles, and of the two-particle propagator that is relevant for the $A \pm 2$ excitations

$$g^{II}_{\alpha\beta,\gamma\delta}(\omega) = \sum_{n} \frac{\langle \Psi_0^A | c_\beta c_\alpha | \Psi_n^{A+2} \rangle \, \langle \Psi_n^{A+2} | c_\gamma^\dagger c_\delta^\dagger | \Psi_0^A \rangle}{\omega - (E_n^{A+2} - E_0^A) + i\eta} - \sum_{k} \frac{\langle \Psi_0^A | c_\gamma^\dagger c_\delta^\dagger | \Psi_k^{A-2} \rangle \, \langle \Psi_k^{A-2} | c_\beta c_\alpha | \Psi_0^A \rangle}{\omega - \left(E_0^A - E_k^{A-2}\right) - i\eta} \, . \tag{4}$$

In the calculation of Sec. III, these quantities have been evaluated by solving the dressed TDA/RPA (DTDA/DRPA) equations [20, 21] for the ph and pp case, respectively. The fact that a dressed sp propagator is used brings in to the calculation the effects of the strength distribution for particle and hole fragments. One must notice that the propagators (3) and (4) are in fact the solution of more general Bethe-Salpeter equations, that also include correlations beyond the RPA level. One of these is the mixing of many-phonons in the kernel of the BSE. A first calculation in this direction has been done for the ph propagator $\Pi(\omega)$ [13] and is reported in Sec. IV.

Once one has obtained the ph (3) and pp(hh) (4) propagators, their coupling to the sp motion has to be accounted for in the nuclear self-energy. To do this the 2p1h and 2h1p propagators of Fig. 1 are computed by solving a set of Faddeev equations [22, 23]. The details of the formalism employed in this calculation have been discussed in Ref. [14] and will not be shown here. For the present discussion it is sufficient to note that this approach computes the motion of three-quasiparticle

Shell	TDA	RPA	1st itr.	2nd itr.	3rd itr.	4th itr.
$Z_{p_{1/2}}$	0.775	0.745	0.775	0.777	0.774	0.776
$Z_{p_{3/2}}$	0.766	0.725	0.725	0.727	0.722	0.724
			0.015	0.027	0.026	0.026
Total occ.	14.56	14.56	14.56	14.57	14.58	14.63

TABLE I: Hole spectroscopic factors (Z_α) for knockout of a $\ell = 1$ proton from ^{16}O. These results refer to the initial IPM calculation and the first four iterations of the DRPA equations. All the values are given as a fraction of the corresponding IPM value. Also included is the total number of nucleons, as deduced from the complete one-hole spectral function, for each iteration.

excitations in the same way it is normally done to solve the three-body problem. This allows to include the effects of ph and pp(hh) motion not only at the TDA level but also with more collective RPA phonons and beyond. Such excitations are coupled to each other by the Faddeev equations, generating an infinite series of diagrams like the one shown in Fig. 2. Moreover, Pauli correlations are properly taken into account at the 2p1h/2h1p level.

III. RESULTS FOR THE SINGLE-PARTICLE SPECTRAL FUNCTION OF ^{16}O

In the calculations described below, the Dyson equation was solved within a model space consisting of harmonic oscillator sp states. An oscillator parameter $b = 1.76$ fm was chosen (corresponding to $\hbar\omega = 13.4$ MeV) and all the first four major shells (from $1s$ to $2p1f$) plus the $1g_{9/2}$ where included. Inside this model space, the interaction used was a Brueckner G-matrix [24] derived from the Bonn-C potential [25]. The results of Refs. [5, 13], suggest that this model space is large enough to properly account for the low-energy collective states in which we are mainly interested in, the SRC being accounted for through the G-matrix effective interaction. We note that energy dependence of the G-matrix also contributes to the normalization of the spectral strength. In Ref. [11], it was shown that this accounts for the extra depletion of spectroscopic factors that is induced by SRC, at least for the normally occupied shells in the IPM.

We mention that the solution of RPA equations may lead to collective instabilities whenever the iteration becomes too attractive. A particular sensitivity to the strength of the G-matrix interaction was found in the calculation of [12], only for the lowest isoscalar 0^+ solution. For this reason it was chosen to artificially shift its eigenvalue to the experimental energy of first excited state, 6.05 MeV, during the successive iterations. Note that the screening due the redistribution of the sp strength tends to reduce the instability problem in DRPA. Moreover, the origin of the instability for this particular solution has been identified and corrected later, in Ref. [13].

A. Effects of RPA correlations and fragmentation

For an IPM ansatz the TDA calculation is equivalent to the one of Ref. [11] and yields the same result for the spectroscopic factors of the main particle and hole shells close to the Fermi energy. These correspond to 0.775 for $p_{1/2}$ and 0.766 for $p_{3/2}$ and are reported in Table I. The introduction of RPA correlations reduces these values and brings them down to 0.745 and 0.725, respectively. This result reduces the discrepancy with the experiment by about 4% and shows that collectivity

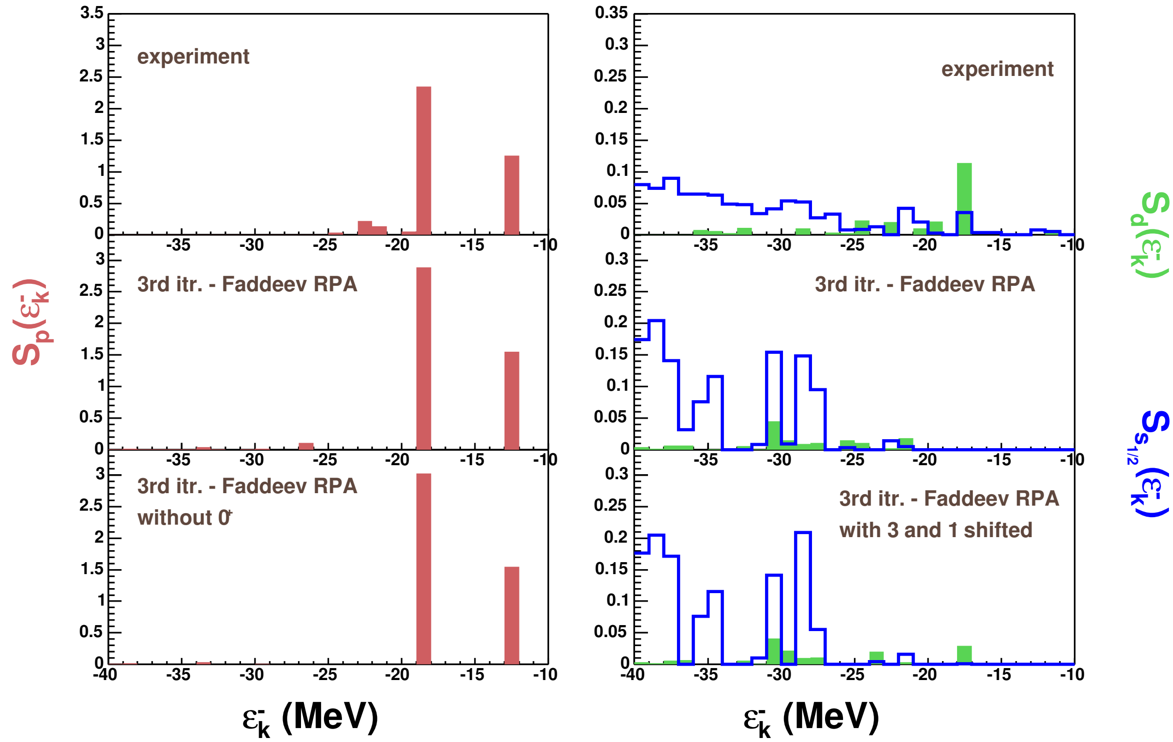

FIG. 3: One-proton removal strength as a function of the hole sp energy $\varepsilon_k^- = E_0^A - E_k^{A-1}$ for ^{16}O for angular momentum $\ell = 1$ (left) and $\ell = 0, 2$ (right). For the positive parity states, the solid bars correspond to results for $d_{5/2}$ and $d_{3/2}$ orbitals, while the thick lines refer to $s_{1/2}$. The top panels show the experimental values taken from [3]. The mid panels give the theoretical results for the self-consitent spectral function. The bottom panels show the results obtained by repeating the 3$^{\rm rd}$ iteration with a modified ph-DRPA spectrum, in which the lowest eigenstates have been shifted to the corresponding experimental values.

beyond the TDA level is relevant to explain the quenching of spectroscopic factors. Since the present formalism does not account for center-of-mass effects, the above quantities need to be increased by about 7% before they are compared with the experiment [26].

The RPA results were iterated a few times, with the aim of studying the effects of fragmentation on the RPA phonons and, subsequently, on the spectral strength. Since we are looking at low-energy excitations, it is sufficient to keep track only of the most occupied fragments that appear —close to the Fermi energy— in the (dressed) sp propagator, Eq. (1), while the residual strength is collected in a effective pole [12, 27]. As shown in Table I, only a few iterations are required to reach convergence. The converged distribution of one-hole strength is compared in with the experimental one in Fig. 3. The main difference between these results and the one obtained by using an IPM input is the appearance of a second smaller $p_{3/2}$ fragment at -26.3 MeV. This peak arises in the first two iterations and appears to become stable in the last one, with a spectroscopic factor of 2.6%. This can be interpreted as a peak that describes the fragments seen experimentally at slightly higher missing energy. This is the first time that such a fragment is obtained in calculations of the spectral strength. Further insight into the appearance of this strength is discussed in Sec. III B.

A second effect of including fragmentation in the construction of the RPA phonons is to increase the strength of the main hole peaks. The $p_{1/2}$ strength increases from the 0.745 obtained with IPM input to 0.776, essentially canceling the improvement gained by the introduction of RPA correlations over the TDA ones. The main peak of the $p_{3/2}$ remains at 0.722 but the appearance of the secondary fragment slightly increases the overall strength at low energy as well. This behavior is due to the fact that redistribution of the strength (and principally, the reduction of the main spectroscopic factors) tends to screen the nuclear interaction, with respect to the IPM case. Obviously, this makes the disagreement with experiments a little worse and additional work is needed to resolve the disagreement with the data. Nevertheless it is clear that fragmentation is a relevant feature of nuclear systems and that it has to be properly taken into account.

Together with the main fragments, the Dyson equation produces also a large number of solutions with small spectroscopic factors. This strength extends down to about -130 MeV for the one-hole spectral function and up to about 100 MeV for the one-particle case. This background represents the strength that is removed from the main peaks and shifted up to medium missing energies. Another 10% of strength is moved to very high energies due to SRC [9]. Its location cannot be explicitly calculated in the present approach but the effects on the reduction of spectroscopic factors at low energy is accounted through the energy dependence of the G-matrix. Accordingly the total number of nucleons deduced from the fully self-consistent spectral function is about a 10% lower than $A = 16$, as reported in Table I.

We note that the present approach gives predictions also for the strength distribution of quasiparticle excitations. Although little experimental information is available for the addition of a nucleon (as well as for the removal of a neutron). Recently, knockout and nucleon transfer reactions, employing nuclear probes, have been applied to measure the hole spectroscopic factors of both stable and exotic nuclei [28, 29]. These tools can now reach better accuracies than in the past and may, in principle, be used to extract information on the one-particle spectral distribution.

B. Role of 0^+ and 3^- excited states in ^{16}O

A deeper insight into the mechanisms that generate the fragmentation pattern can be gained by investigating directly the connection between the spectral function and some specific collective states. To clarify this point we repeated the third iteration using exactly the same input but without keeping the troublesome ph 0^+ state at its experimental energy, it was discarded instead. The resulting p hole spectral function is shown in the lower-left panel of Fig. 3. In this calculation no breaking of the $p_{3/2}$ strength is obtained but only a single peak is found with a spectroscopic factor equal to 0.75, which is the sum of the two fragments that are obtained when the 0^+_2 state is taken into account. This result can be interpreted by considering the $p_{3/2}$ fragments as a hole in the ground state and in the first excited 0^+ state of the ^{16}O core, respectively. The correct fragmentation pattern can be reproduced only when latter two levels are close enough, in energy, to one another.

The other two low-lying states of ^{16}O that may be of some relevance are the isoscalar 1^- and 3^-. These excitations are reproduced reasonably well by RPA type calculations [30] but are typically found at $\sim$3 MeV above the experimental results. The lower panels of Fig. 3 show the results for the even parity spectral functions that are obtained when both the 3^- and the 1^- ph-DRPA solutions are shifted to match their experimental values. In this case, a $d_{5/2}$ hole peak is obtained at a missing energy -17.7 MeV, in agreement with experiment, and with a spectroscopic strength of 0.5%.

It should be noted that many *weak* fragments (i.e. relative to the addition or knockout for a nucleon with a small spectroscopic factor) are seen throughout the nuclear table of isotopes. Most of these have no direct explanation in terms of mean-field sp states and contain more complicated components, involving 2p1h/2h1p configurations and beyond. Jennings and Escher have shown that different definitions of the overlap wave function can be given that completely describe the sp motion inside the nuclear medium. Although, each of them sample the Pauli correlations in a different way, resulting in very different normalizations of the amplitudes of weak states [31]. This may have important consequences for the reliability of spectroscopic factors extracted from proton emission

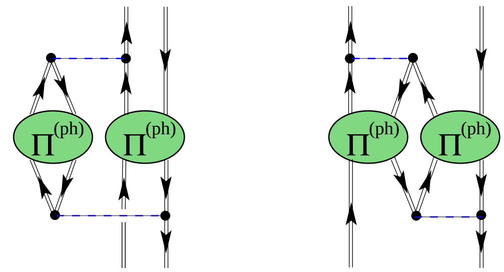

FIG. 4: Examples of contributions involving the coupling of two independent ph phonons. In total, there are sixteen possible diagrams of this type, obtained by considering all the possible couplings to a ph state. The two-phonon ERPA equations sum all of these contributions in terms of dressed sp propagators.

and pick-up/stripping reactions [32].

IV. EXTENSION OF RPA AND SPECTRUM OF ^{16}O

The above results suggest that the main impediment for further improvements of the description of the experimental spectral strength is associated with the deficiencies of the RPA (DRPA) description of the excited states. One important problem is the appearance of at most one collective phonon for a given J^π, T combination while several low-lying isoscalar 0^+ and 2^+ excited states are observed at low energy in ^{16}O, as well as additional 3^- and 1^- states. A possible way to proceed would be to first concentrate on an improved description of the collective phonons by extending the RPA to explicitly include the coupling to two-particle−two-hole (2p2h) states. Such an extended RPA procedure has been applied in heavier nuclei with considerable success [5]. In order to be relevant for ^{16}O, this approach requires an extension in which the coherence of the 2p2h states is included in the form of the presence of two-phonon excitations [33]. This correspond to adding two-phonon configurations to the kernel of the BSE for the ph propagator (3), as shown in Fig. 4 [13].

We note that there has been a tremendous progress in recent years in the microscopic description of p shell nuclei using Green's Function Monte Carlo and no-core shell model methods [38, 39]. A possible application of the no-core shell model to ^{16}O would properly include the 4p4h effects relevant for describing the spectrum of ^{16}O [40]. However the description of spectroscopic factors will require the construction of effective operators to include the effects of short-range correlations on these quantities whereas they are automatically included in the SCGF method. Whence the interest in studying the spectrum of ^{16}O with the present method.

The formalism to include two-phonon configurations has been presented in Ref. [13], where it is referred as two-phonon extended RPA (ERPA). In this work the ph-DRPA equation has been solved first, using the self-consistent sp propagator derived in Sec. III. The lowest DRPA solutions for both the 0^+, 3^- and 1^- channels were shifted down to their relative experimental energies and then they were employed to generate the two-phonon contributions for the ERPA calculation. The spectrum obtained for ^{16}O is displayed in Fig. 5 and Table II together the total ph strength Z_{n_π} of each state,

$$Z_{n_\pi} \;=\; \sum_{\alpha\beta} \left| \langle \Psi^A_{n_\pi} | c^\dagger_\alpha c_\beta | \Psi^A_0 \rangle \right|^2 \; . \tag{5}$$

Table II also reposts the relative occupation of ph and two-phonon admixtures in the wave function for each solution of the ERPA equation.

The results yield an isoscalar 0^+ state with a predominant ph character at ∼17 MeV, as it was found in DRPA. Although this solution is now characterized by a partial mixing with two-phonon configurations. Table II shows that this is the result of mixing with the lowest solution in the same channel, which ends up at ∼11 MeV. The latter is predominately a two-phonon state. It is also seen that in both cases the relevant configuration comes from the coupling of two 0^+ phonons

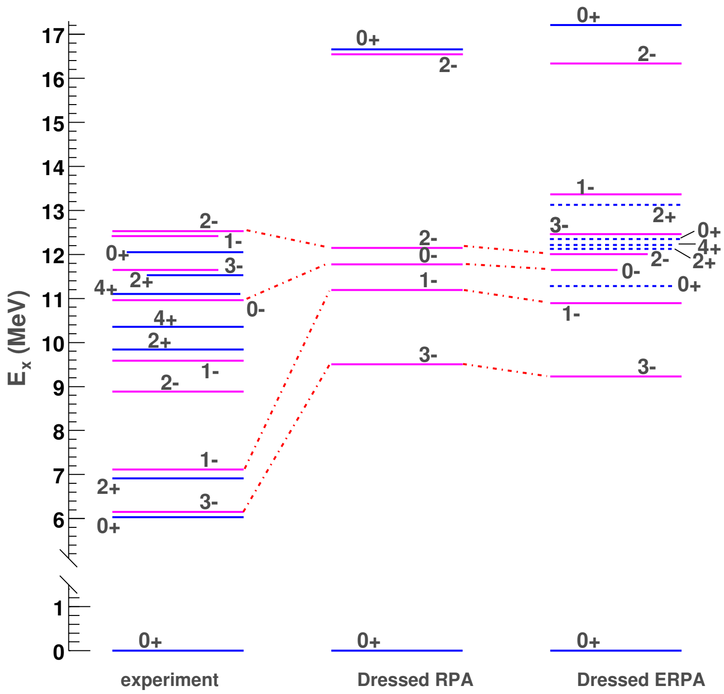

FIG. 5: Results for the DRPA and the two-phonon ERPA propagator of ^{16}O with the dressed input propagator computed in Sec. III, middle and last column respectively. In solving the ERPA equation, the lowest 3^-, 1^- and 0^+ levels of the DRPA propagator where shifted to their experimental energies. All other DRPA solutions were left unchanged. The excited states indicated by dashed lines are those for which the (E)RPA equation predicts a total spectral strength Z_{n_π} lower than 10%. The first column reports the experimental results [34].

themselves. The calculations of Ref. [35] have shown that the bulk of the 4p4h contributions to the first excited state of ^{16}O may come from the coupling of four different phonons with negative parity (3^- and 1^-). However, the self-consistent role of coupling positive parity states was not considered in that work. Both this effect, the RPA correlations and the inclusion of the nuclear fragmentation allow for the –at least partial– inclusion of configurations beyond the 2p2h case even when no more than two-phonon coupling is considered, as in this paper. A study of the importance of three- and four-phonon configurations will be addressed in the future.

The low-lying negative parity isoscalar states (3^- and 1^-) are only slightly affected by two-phonon contributions and remain substantially above the experimental energy at 9.23 and 10.90 MeV, respectively, and more correlations will be needed in order to lower their energy. We note that these wave functions contain a two-phonon admixture obtained by coupling the low-lying 0^+ excitation to either the 3^- or 1^- phonons. According to the above interpretation of the first 0^+ excited state this corresponds to the inclusion of 3p3h and beyond. At the same time two additional negative parity solutions, with two-phonon character, are found at higher energy in accordance with experiment.

The two-phonon ERPA approach also generates a triplet of states at about 12 MeV, with quantum numbers 0^+, 2^+ and 4^+. A similar triplet is found experimentally at 12.05, 11.52 and 11.10 MeV, which also corresponds to twice the experimental energy of the first 3^- phonon. The ERPA solutions for this triplet are almost exclusively obtained by $3^-\otimes 3^-$ states and therefore have a 2p2h character, in accordance with Refs. [36, 37]. Further interaction in the pp and hh channels will be needed in order to reproduce the correct experimental splitting and experimental strength [35].

V. CONCLUSIONS

In the present paper the Faddeev technique, combined with self-consistent Green's Function theory, has been applied to study 2h1p correlations at small missing energies for the nucleus of ^{16}O. The

$T=0$	dressed/DRPA		dressed/ERPA				$(0_2^+)^2$	$(3_1^-)^2$	$(0_2^+,3_1^-)$	$(0_2^+,1_1^-)$
J^π	ε_n^π	Z_{n_π}	ε_n^π	Z_{n_π}	ph(%)	2Π(%)	(%)	(%)	(%)	(%)
1^-			13.37	0.148	21	79				79
3^-			12.35	0.113	16	84			84	
0^+			12.15	0.001	1	99	3	96		
4^+			12.14	0.007	1	99		99		
2^+			12.12	0.008	1	99		98		
0^+	16.62	0.717	17.21	0.633	88	12	10	0.5		
0^+			11.28	0.092	12	88	85	2		
1^-	11.19	0.720	10.90	0.680	94.1	5.9				5.8
3^-	9.50	0.762	9.23	0.735	95.9	4.1			4.0	

TABLE II: Excitation energy and total spectral strengths obtained for the principal solutions of DRPA and two-phonon ERPA equations. The total contribution of ph and two-phonon states of the ERPA solutions are shown. For states below 15 MeV, the columns on the right side give the individual contributions of all the relevant two-phonon contributions.

application of the Faddeev method allows for the first time the treatment of the coupling of ph and pp(hh) collective modes within a RPA framework, while the effects of fragmentation are included through the dressing of the sp propagator. The present approach allows to further identify the important role played by the low-lying excited states of ^{16}O. These are seen to be essential to generate many of the fragments with small spectrocopic factors that are seen experimentally, like the $s_{1/2}$ and $p_{3/2}$ states of ^{15}N at 5.20 MeV and ∼9 MeV. .

The main impediment in obtaining a good theoretical description of the single particle spectral function of ^{16}O has been identified in the poor description of the excitation spectrum, as obtained by solving the standard (D)RPA equations. We have improved on this by computing the effects of mixing of ph states with two-phonon configurations in the kernel of the Bethe-Salpeter equations. Moreover, configurations beyond the 2p2h level were also partially included by means of improved RPA and self-consistency effects. The results show that these contributions explain the formation of several excited states observed at low energy which are not obtained by RPA calculations. Still it appears that a full solution of the spectrum of ^{16}O with this method requires to consider the mixing of up to four phonons and the interaction in the pp and hh channels [35]. The inclusion of such effects will be the topic of future work.

Acknowledgments

One of us (C.B.) acknowledge useful discussions with J.-M. Sparenberg and B. Jennings. This work was supported in part by the U.S. National Science Foundation under Grants No. PHY-9900713 and PHY-0140316 and in part by the Natural Sciences and Engineering Research Council of Canada (NSERC).

[1] V. R. Pandharipande, I. Sick and P. de Witt Huberts, Rev. Mod.. Phys. **69**, 981 (1997).
[2] L. Lapikás, Nucl. Phys. **A553**, 297c (1993); I. Sick and P. de Witt Huberts, Commun. Nucl. Part. Phys. **20**, 177 (1991).
[3] M. Leuschner *et al.*, Phys. Rev. C **49**, 955 (1994).

[4] D. Rohe, in Proc. Fifth Workshop on *Electromagnetically induced two-hadron emission*, eds. P. Grabmayr *at al.* (Univ. Lund, published on CD, ISBN: 91-631-1612-X, 2001), p. 67.

[5] M. G. E. Brand, K. Allaart, and W. H. Dickhoff, Phys. Lett. **B214**, 483 (1988); M. G. E. Brand, K. Allaart, and W. H. Dickhoff, Nucl. Phys. **A509**, 1 (1990). M. G. E. Brand, G. A. Rijsdijk, F. A. Muller, K. Allaart, and W. H. Dickhoff, *ibid.* **A531**, 253 (1991); G. A. Rijsdijk, K. Allaart, and W. H. Dickhoff, *ibid.* **A550**,159 (1993)

[6] L. Lapikás, J. Wesseling, and R. B. Wiringa Phys. Rev. Lett. **82**, 4404-4407 (1999).

[7] H. Müther and W. H. Dickhoff, Phys. Rev. C **49**, R17 (1994); H. Müther, W. H. Dickhoff and A. Polls,, *ibid.* **51**, 3040 (1995).

[8] M. Radici, S. Boffi, S C. Pieper, and V. R. Pandharipande, Phys. Rev. C **50**, 3010 (1994); A. Fabrocini and G. Co', *ibid.* **63**, 044319 (2001).

[9] B. E. Vonderfecht, W. H. Dickhoff, A. Polls, and A. Ramos, Phys. Rev. C **44**, R1265 (1991).

[10] K. Amir-Azimi-Nili, H. Müther, L. D. Skouras, and A. Polls, Nucl. Phys. **A604**, 245 (1996); Kh. Gad and H. Müther, Phys. Rev. C **66**, 044301 (2002).

[11] W. J. W. Geurts, K. Allaart, W. H. Dickhoff, and H. Müther, Phys. Rev. C **53**, 2207 (1996).

[12] C. Barbieri and W. H. Dickhoff, Phys. Rev. C **65**, 064313 (2002).

[13] C. Barbieri and W. H. Dickhoff, Phys. Rev. C **68**, 0143xx (2003).

[14] C. Barbieri and W. H. Dickhoff, Phys. Rev. C **63**, 034313 (2001).

[15] C. Barbieri and W. H. Dickhoff, in Proc. Fifth Workshop on *Electromagnetically induced two-hadron emission*, eds. P. Grabmayr *at al.* (Univ. Lund, published on CD, ISBN: 91-631-1612-X, 2001), p. 108.

[16] A. L. Fetter and J. D. Walecka, *Quantum Theory of Many-Particle Physics* (McGraw-Hill, New York, 1971).

[17] A. A. Abrikosov, L. P. Gorkov and I. E. Dzyaloshinski, *Methods of Quantum Field Theory in Statistical Physics* (Dover, New York, 1975).

[18] J. Winter, Nucl. Phys. **A194**, 535 (1972).

[19] G. Baym and L. P. Kadanoff, Phys. Rev. **124**, 287 (1961).

[20] P. Ring and P. Schuck, *The Nuclear Many-body Problem* (Springer, New York, 1980).

[21] G. A. Rijsdijk, W. J. W. Geurts, M. G. E. Brand, K. Allaart, and W. H. Dickhoff, Phys. Rev. C **48**, 1752 (1993); W. J. W. Geurts, K. Allaart, and W. H. Dickhoff, Phys. Rev. C **50**, 514 (1994).

[22] L. D. Faddeev, Zh. Éksp. Teor. Fiz. **39** 1459 (1961) [Sov. Phys. JETP **12**, 1014 (1961)].

[23] W. Glöckle, *The Quantum Mechanical Few-Body Problem* (Springer, Berlin, 1983).

[24] H. Müther and P. Sauer, in *Computational Nuclear Physics* ed. by K.-H. Langanke, et al. (Springer Berlin, 1993).

[25] R. Machleidt, Adv. Nucl. Phys. **19**, 191 (1989).

[26] A. E. L. Dieperink and T. de Forest, Jr. Phys Rev. C **10**, 543 (1974); D. Van Neck, M.Waroquier, A. E. L. Dieperink, S C. Pieper, and V. R. Pandharipande, *ibid.* **57**, 2308 (1998).

[27] J. Yuan, Ph.D. thesis, Washington University, St. Louis, 1994.

[28] G. J. Kramer, H. P. Blok, and L. Lapikás, Nucl. Phys. **A679**, 267 (2001).

[29] B. A. Brown, P. G. Hansen, B. M. Sherill, and J. A. Tostevin, Phys. Rev. C **65**, 061601(R) (2002); P. G. Hansen, proceedings of this workshop.

[30] P. Czerski, W. H. Dickhoff, A. Faessler, and H. Müther, Phys. Rev. C **33**, 1753 (1986).

[31] J. Escher and B. K. Jennings, Phys. Rev. C **66**, 034313 (2002).

[32] J. Al-Khalili, C. Barbieri, J. Escher and B. K. Jennings, and J.-M. Sparenberg, nucl-th/0304055; To be published on Phys. Rev. C.

[33] W. H. Dickhoff, in *Condensed Matter Theories. Vol. 3*, ed. J. S. Arponen, R. F. Bishop and M. Manninen (Plenum, New York 1988) p. 261.

[34] F. Ajzenberg-Selove, Nucl. Phys. **A375**, 1 (1982).

[35] H. Feshbach and F. Iachello, Phys. Lett. **B45**, 7 (1973); H. Feshbach and F. Iachello, Ann. Phys. **84**, 211 (1974).

[36] T. N. Buti *et al.*, Phys. Rev. C **33**, 755 (1986).

[37] M. S. Zisman, E. A. McClatchie, and B. G. Harvey, Phys. Rev. C **2**, 1271 (1970); J. Lowe and A. R. Barnett, Nucl. Phys. **A187**, 323 (1972).

[38] B. S. Pudliner, V. R. Pandharipande, J. Carlson, S. C. Pieper, and R. B. Wiringa, Phys. Rev. C **56**, 1720 (1997); S. C. Pieper, K. Varga, and R. B. Wiringa, Phys. Rev. C **66**, 044310 (2002).

[39] P. Navrátil, J. P. Vary, and B. R. Barrett, Phys. Rev. C 62, 054311 (2000); P. Navrátil and B. R. Barrett, Phys. Rev. C 57, 3119-3128 (1998); P. Navrátil and W. E. Ormand, Los Alamos archive: nucl-th/0305090.

[40] G. E. Brown, and A. M. Green, Nucl. Phys. **75**, 401 (1966); W. C. Haxton, and C. J. Johnson, Phys. Rev. Lett. **65**, 1325 (1990); E. K. Warburton, B. A. Brown, and D. J. Millener, Phys. Lett. **B293**, 7 (1992).